

Deletion Analysis of Two Tandemly Arranged Virulence Genes in Myxoma Virus, M11L and Myxoma Growth Factor

ANDREA OPGENORTH,¹ KATHRYN GRAHAM,¹ NICK NATION,² DAVID STRAYER,³
AND GRANT MCFADDEN^{1*}

Department of Biochemistry,¹ and Health Sciences Lab Animal Services,² University of Alberta, Edmonton, Alberta, Canada T6G 2H7, and Department of Pathology and Laboratory Medicine, University of Texas Health Science Center, Houston, Texas 77030³

Received 29 August 1991/Accepted 28 April 1992

Myxoma virus (MYX) is a leporipoxvirus of rabbits that induces a lethal syndrome characterized by disseminated tumorlike lesions, generalized immunosuppression, and secondary gram-negative bacterial infection. A MYX deletion mutant (vMYX-GF⁻ΔM11L) was constructed to remove the entire myxoma growth factor (MGF) coding sequence and that for the C-terminal five amino acids of the partially overlapping upstream gene, M11L. Unexpectedly, this deletion completely abrogates the capacity of MYX to cause the characteristic disease symptoms of myxomatosis. Upon inoculation of rabbits with vMYX-GF⁻ΔM11L, recipient animals developed only a benign, localized nodule reminiscent of a Shope fibroma virus-induced tumor in which a single primary lesion appeared at the site of injection and then completely regressed within 14 days, leaving the animals resistant to challenge with wild-type MYX. No evidence of the purulent conjunctivitis and rhinitis that always accompany wild-type MYX infection was observed. To ascertain whether the attenuation observed in vMYX-GF⁻ΔM11L was due to a combined effect of the MGF deletion and alteration of the upstream M11L gene, two additional MYX recombinants were constructed: an MGF⁻ virus (vMYX-GF⁻) containing an intact M11L gene and an M11L⁻ virus (vMYX-M11L⁻) containing an intact MGF gene. Infection with vMYX-GF⁻ resulted in moderated symptoms of myxomatosis, but all clinical stages of the disease were still detectable. In contrast, disruption of M11L alone dramatically reduced the virus virulence, resulting in a nonlethal syndrome whose clinical course was nevertheless distinct from that of vMYX-GF⁻ΔM11L. Upon inoculation with vMYX-M11L⁻, rabbits developed primary and secondary tumors which were larger and more circumscribed than those of wild-type MYX recipients. Whereas wild-type MYX infection always includes severe, purulent conjunctivitis and rhinitis, vMYX-M11L⁻ recipients remained healthy and displayed only minimal signs of respiratory distress. By about 30 days after infection, the tumors induced by vMYX-M11L⁻ had completely regressed and these animals were immune to challenge with wild-type MYX. Histological analysis indicated that tumors induced by vMYX-M11L⁻ are much more heavily infiltrated with macrophages and heterophils and that the sites of viral replication are more edematous and necrotic than those of wild-type infection, suggesting that the host was able to mount a more vigorous inflammatory response to vMYX-M11L⁻ infection. Although vMYX-GF⁻ΔM11L and vMYX-M11L⁻ propagated efficiently in vitro in susceptible rabbit and primate fibroblast cell lines, a major defect in the replication of both viruses in primary mixed rabbit spleen cell cultures was noted. We conclude that the M11L gene product is an important virulence determinant for MYX and that the inability of vMYX-GF⁻ΔM11L to cause disease was due to the combined disruption of two distinct virulence factors, MGF and M11L.

The *Poxviridae* is a very large family of DNA viruses whose members have been isolated from most vertebrate species and some insects (15, 33). They produce a remarkably diverse spectrum of disease pathologies in their infected hosts and encode many products which are nonessential for viral replication but directly or indirectly affect virulence, host range, and tissue tropism (7, 54, 55). Examples of such poxviral products include epidermal growth factor homologs (4, 12, 36, 37, 56-58), serine protease inhibitors (serpins) (2, 27, 35, 43, 60), soluble forms of the tumor necrosis factor alpha receptor (42, 59), and an inhibitor of the classical complement pathway (25, 26).

Despite the cytoplasmic site of poxviral replication and assembly, a number of poxviruses are considered to be tumorigenic because they cause extensive cellular proliferation at or near sites of viral replication (14, 15, 32). Some of these tumorigenic poxviruses are also able to induce a lethal,

invasive disease syndrome due to concomitant immune dysfunction brought about in part by the ability to replicate in, and interfere with the normal function of, host lymphocytes (32, 44). One example is myxoma virus (MYX), the causative agent of myxomatosis, which, because of its extreme virulence and narrow host range, was deliberately released in Australia in 1950 to facilitate control of the European rabbit (*Oryctolagus cuniculus*) population. The epidemiology and pathological effects of MYX on feral rabbit populations have been studied in detail (17, 18, 32).

Characterization of the 160-kb MYX genome (1, 38) has shown that it is organized in a fashion similar to that of other poxviruses in that it contains cross-linked termini, terminal inverted repeats (TIR), and an estimated coding capacity for over 200 gene products. Despite the variation in degree of virulence in different strains of MYX, their restriction enzyme cleavage maps are relatively well conserved (38). MYX is very closely related to other members of the *Leporipoxvirus* genus, such as Shope fibroma virus (SFV). Analysis of several open reading frames (ORFs) encoded

* Corresponding author.

within the TIR of MYX reveals a high degree of conservation with the SFV ORF counterparts, both at the nucleotide (nt; >75%) and amino acid (aa; >80%) levels (57–59). Malignant rabbit fibroma virus (MRV) is an SFV/MYX recombinant virus in which approximately 7 kb of MYX sequences near the left terminus was deleted and replaced with homologous SFV sequences, and a 4-kb subset of this was substituted for MYX sequences at the right terminus (1, 45, 57). Thus, MRV is 95% identical to MYX, except for the acquisition of five genes from SFV plus the generation of three MYX/SFV fusion genes. The syndrome induced by MRV has been examined in detail, and because of its similarity to MYX infection, it is believed that results of studies on MRV are generally applicable to MYX as well (7, 32, 44). Upon intradermal (i.d.) infection with even very low doses of MRV or MYX, recipients develop a primary tumorlike lesion which disseminates throughout the dermis and subcutis to multiple external and internal tissues. Dissemination of the virus to secondary sites by productively infected lymphocytes is accompanied by profound generalized immunosuppression and concomitant secondary bacterial infections which cause purulent conjunctivitis and rhinitis, leading to dyspnea and death within 10 to 14 days. The pathological effects of MYX and MRV have been well characterized (17, 18, 31, 45, 48), but the molecular mechanisms by which these viruses induce tumor formation and immunosuppression remain to be established (32, 44, 49).

Most, if not all, poxviruses encode products that are members of the epidermal growth factor (EGF) family of growth factors (4, 12, 36, 37, 56–58). The prototype of this family, vaccinia growth factor (VGF), is modified by proteolytic cleavage and glycosylation and is secreted from vaccinia virus-infected cells. The fully mature VGF ligand has been shown to compete with EGF for binding to the EGF receptor at the cell surface, to be mitogenic for responsive cell types bearing the EGF receptor, and to play a role in vaccinia virus pathogenicity (5–7, 24, 53, 56). The EGF analog encoded by MRV is one of the five gene products derived from SFV sequences and is designated Shope fibroma growth factor (SFGF) (12, 57). Whereas wild-type MRV infection in the European rabbit is 100% fatal, even with very small inocula, 75% of rabbits infected with MRV containing an SFGF deletion (MRV-GF⁻) undergo a less severe disease course and completely recover from infection (34). In addition, the primary and secondary tumors induced by MRV-GF⁻ display a reduced degree of cellular hyperplasia compared with those of wild-type MRV recipients, particularly in the nasal mucosa and conjunctiva (34). MYX contains a related but distinct EGF-like gene, called myxoma growth factor (MGF), which is 80% conserved with SFGF (58). During the course of our studies to ascertain whether the biological roles of MGF in MYX infection are comparable to those of SFGF in MRV infection, we constructed a deletion mutant of MYX (vMYX-GF⁻ΔM11L) in which the entire 460-bp MGF coding sequence was deleted from the genome. Unexpectedly, this single deletion resulted in a drastic attenuation of MYX that was far more profound than that predicted by our studies on the SFGF deletion in MRV, and in fact, the ability to induce virtually all the symptoms of myxomatosis was abrogated. Fine analysis of the deletion construct used to produce this MYX mutant revealed that the manipulation also resulted in the removal of the carboxy terminus of the partially overlapping upstream ORF, designated M11L. M11L encodes a potential 166-aa polypeptide whose carboxy terminus overlaps the amino terminus of MGF by six residues (58). Here we show

that M11L and MGF are two independent virulence factors in MYX and that mutations in both genes simultaneously result in the complete loss of viral pathogenicity in rabbits.

MATERIALS AND METHODS

Cells and virus. Rabbit SIRC cells were obtained from the American Type Culture Collection and maintained in Dulbecco modified Eagle's medium (DMEM) supplemented with 10% fetal bovine serum. RK-13 cells (provided by S. Sell) and BGMK cells (provided by S. Dales) were grown in DMEM supplemented with 10% newborn calf serum. The Lausanne strain of MYX used in this study (3, 16, 17) was obtained from the American Type Culture Collection.

Enzymes and chemicals. Restriction enzymes were supplied by Bethesda Research Laboratories, Inc., Boehringer Mannheim Biochemicals, and New England Biolabs. T4 DNA polymerase, T4 DNA ligase, calf intestinal phosphatase, and 5-bromo-4-chloro-3-indolyl-β-D-galactopyranoside (X-Gal) were purchased from Boehringer Mannheim. The *KpnI* and *BglII* linkers were obtained from the Regional DNA Synthesis Laboratory, University of Calgary. Lipofectin was obtained from Bethesda Research Laboratories.

Plasmid constructs. A 4.5-kb *SmaI* fragment containing the MGF gene was isolated from the MYX 8.6-kb *BamHI* fragment E, which maps at the left end of the viral genome and encompasses the unique sequence-TIR border (1, 38), and ligated into the *SmaI* site of pUC13. The resulting plasmid, pMyS2a, was unstable in standard *recA* bacterial strains (e.g., HB101) but could be propagated in DB1256, which contains *recA*, *recBC*, and *sbcb* loci (13). pMyS2a was linearized by digestion with *KpnI*, whose unique enzyme recognition site maps within the first five nt of MGF coding sequences (58). Partial digestion of this DNA with *NruI*, for which there are two sites in pMyS2a, yielded a product in which 460 nt, including the entire MGF coding region, were deleted. The *KpnI-NruI* deletion therefore spanned from the third codon of MGF to a point 37 nt 5' to the start of the downstream M9L gene. The DNA was blunt ended, *KpnI* linkers were added, and the deletion construct was circularized with T4 DNA ligase and used to transform DB1256. The product, designated pMyK-1, was cleaved with *KpnI* and blunt end ligated to a 3.15-kb *BglII* fragment containing the *Escherichia coli* β-galactosidase gene under the control of the vaccinia p11 promoter (β-gal cassette) (5). The DNA was used to transform DB1256, and a plasmid (pMyPL-5) was isolated in which sequences encompassing the entire MGF gene and the C-terminal five aa of the M11L ORF were deleted and replaced with the β-gal cassette. To create an insertion of the β-gal cassette at a position that did not interrupt any known ORFs, plasmid pMyLac-25 was constructed by blunt ending the *BglII* β-gal cassette into the *SstI* site of pMTL-25 (11) and then excising the β-gal cassette with *KpnI*. This *KpnI*-ended β-gal cassette was then blunt end ligated into the *NruI* site of pMyS2a downstream of the MGF gene, a site which does not interrupt either MGF or M9L (58). To disrupt the MGF gene alone, plasmid pΔMGF-1 was constructed in the following manner: the 1.5-kb *HincII* fragment spanning the MGF gene (58) was blunt end ligated into the *SmaI* site of pMTL23p (11), and the DNA was used to transform *E. coli* JM83 (40). The product, designated pMGF-3, was treated with *BglII*, blunt ended, recircularized in order to destroy the unique *BglII* site in the vector sequences, and used to transform JM83. The product (pMGFB-4) was isolated and cleaved with *BsaBI*, whose unique recognition site (GATNNNNATC) occurs near the

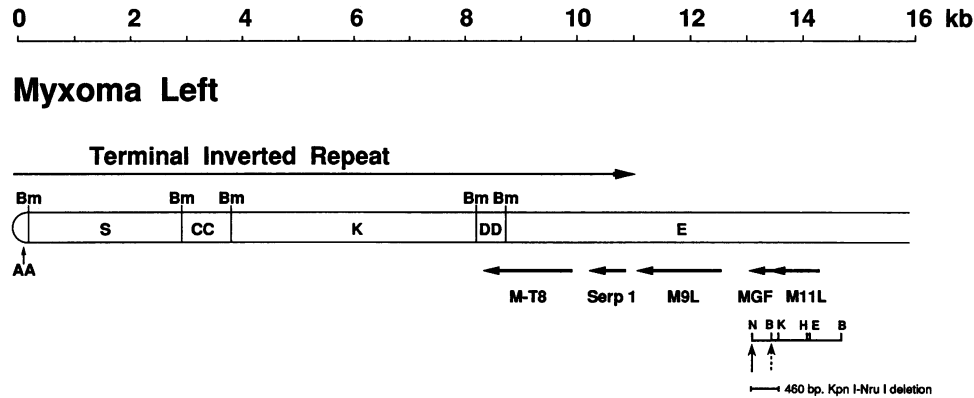


FIG. 1. Diagram of the left end of the MYX genome showing the location of the MGF and M11L ORFs. The *Bam*HI fragments AA, S, CC, K, DD, and E are as described previously (37), except that the orientation has been reversed (see text). The upper arrow denotes the viral TIR, and the lower arrows denote ORFs. The site of the *Kpn*I-*Nru*I 460-bp deletion is indicated. The solid vertical arrow indicates site of β -gal cassette insertion at the *Nru*I site in the control virus vMYXlac. The dashed vertical arrow indicates the site of β -gal cassette insertion at the *Bsa*BI site in vMYX-GF⁻. The site of the *Eco*RV-*Hinc*II deletion in vMYX-M11L⁻ is shown. Abbreviations: Bm, *Bam*HI; B, *Bsa*BI; E, *Eco*RV; H, *Hinc*II; K, *Kpn*I; N, *Nru*I.

middle of the MGF coding sequence (58), *Bgl*III linkers were added, the product was used to transform DB1256, and a plasmid in which the *Bsa*BI site was destroyed and replaced with a *Bgl*III enzyme recognition site (pBsa-7) was isolated. This plasmid was cleaved with *Bgl*III, ligated to the β -gal cassette, and used to transform DB1256, yielding p Δ MGF-1. Plasmid p Δ M11-2 was constructed in the following manner: pMGF-3 was cleaved with *Bgl*III and ligated to the 3.15-kb *Bgl*III β -gal cassette from pSC20. This DNA was used to transform DB1256, and the resulting plasmid was designated pMGF-3lac-7. A 0.9-kb *Eco*RV fragment spanning the 5' end of the M11L gene was isolated from the MYX 8.6-kb *Bam*HI fragment E and ligated into the *Stu*I site of pMGF-3lac-7. Upon transformation of DB1256, p Δ M11-2 with the proper orientation of the M11L 5' sequences was isolated. This plasmid thus contains an M11L coding sequence that has been disrupted by a 52-bp deletion between the *Eco*RV and *Hinc*II sites (Fig. 1) and contains a β -gal marker.

Construction of recombinant viruses. The recombinant viruses were constructed by modified standard procedures used to generate poxvirus mutants (10). Thirty-five-millimeter-diameter dishes of 70% confluent BGMK cells were infected with MYX at a multiplicity of infection (MOI) of 0.05 at 0 h; after 2 h, a calcium phosphate-DNA precipitate containing 500 ng of *Hind*III-linearized pMyLac-25, pMyPL-5, or p Δ MGF-1 was added. At 6 h, the medium was replaced. In the case of vMYX-M11L⁻, at 2 h, the medium was replaced with serum-free DMEM, and a lipofectin-DNA mixture (1:1) containing 1 μ g of *Hind*III-cleaved p Δ M11-2 was added to the medium. At 24 h, the medium was replaced with DMEM-10% newborn calf serum. For all recombinants, at 48 h, the virus was harvested and replated on BGMK cells at a low MOI. After 4 days, recombinant viruses (blue foci or plaques) were identified by overlaying the monolayers with 1% low-melting-point (LMP) agarose in DMEM-5% newborn calf serum containing 500 μ g of X-Gal per ml. For simplicity, both foci and plaques will be generally referred to as plaques. After three cycles of plaque purification under 1% LMP agarose, the stocks were grown to a high titer in RK-13 cells. The genomic structures of candidate recombinant viruses were confirmed by polymerase chain reaction and by Southern blot analysis (not shown) as described previously (22, 62). Recombinant MYX viruses

containing the β -gal cassette at the *Bsa*BI site (vMYX-GF⁻), the β -gal cassette at the *Nru*I site immediately downstream of the MGF gene (vMYXlac), or deleted *Kpn*I-*Nru*I sequences replaced with the β -gal cassette (vMYX-GF⁻ Δ M11L) were identified and the stocks were expanded in RK-13 cells (Fig. 2).

Virus replication analysis in tissue culture. Cultures of RK-13 or SIRC cells in 35-mm-diameter dishes were infected at an MOI of 5 for single-step growth analysis, or 0.002 to generate low-multiplicity growth curves, for 1 h at 37°C in 0.3 ml of DMEM. The inoculum was removed and replaced with DMEM containing the appropriate amount of serum, and the cultures were harvested at various times postinfection (p.i.). When viral growth was studied in growth-arrested cells, the cells were rendered quiescent by reducing the serum content to 0% (RK-13) or 0.2% (SIRC) for 4 days prior to infection. Virus titers were determined by a plaque assay on RK-13 cells and then by X-Gal staining of fixed monolayers. Monolayers of RK-13 cells were fixed in phosphate-buffered saline (PBS) containing 0.02% glutaraldehyde, 1% formaldehyde, and 0.02% Nonidet P-40 (NP-40) at room temperature for 5 min; washed 2 times with PBS; and then stained with 300 μ g of X-Gal per ml in PBS containing 5 mM potassium ferricyanide, 5 mM potassium ferrocyanide, and 1 mM MgCl₂, for 30 min at 37°C (41).

Primary rabbit spleen cell cultures. Spleen cell suspensions from normal and virus-infected rabbits were prepared as described previously (47). Briefly, cells were suspended by passage through a steel mesh and cultured in 96-well, flat-bottom microtiter plates (Costar) at a concentration of 10⁵ per well in 200 μ l of RPMI 1640 (GIBCO) supplemented with 10% fetal bovine serum, L-glutamine (2 mM), 50 μ M 2-mercaptoethanol, and antibiotics. Where present, concanavalin A (conA) and virus were added to the cultures at the time of culture initiation.

Infection of rabbits with MYX, vMYXlac, vMYX-GF⁻, vMYX-GF⁻ Δ M11L, and vMYX-M11L⁻. Adult female New Zealand White rabbits (2.5 to 3 kg) were purchased from local suppliers. They were housed and maintained according to standard procedures. Rabbits were inoculated i.d. in the thigh with doses ranging from 10² to 10⁶ PFU in 1 ml of normal saline; monitored daily for external signs of developing myxomatosis, including the appearance of tumors,

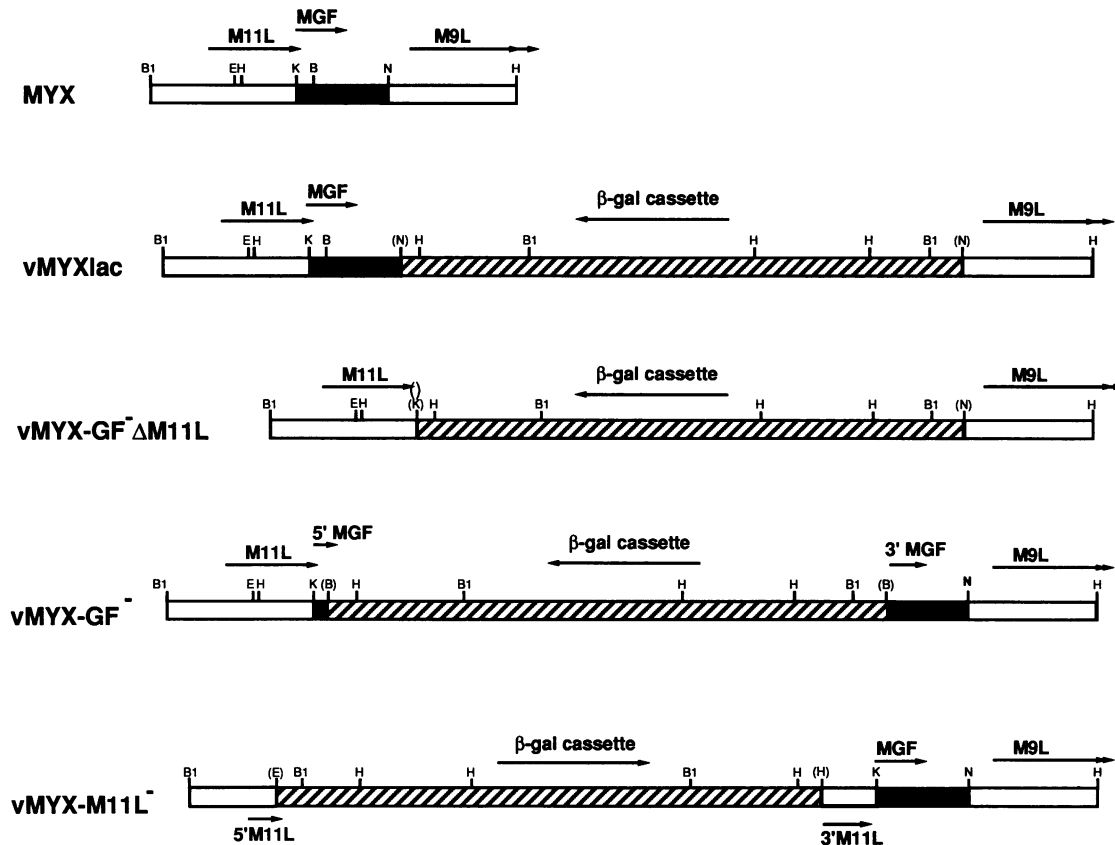


FIG. 2. Structures of MYX, vMYXlac, vMYX-GF⁻ΔM11L, vMYX-GF⁻, and vMYX-M11L⁻ genomes near the MGF locus. The orientations are reversed from those seen in Fig. 1. Abbreviations: B1, *Bgl*I; B, *Bsa*BI; E, *Eco*RV; H, *Hinc*II; K, *Kpn*I; N, *Nru*I.

febrility, conjunctivitis, and rhinitis; and sacrificed with euthanyl administered intravenously after anaesthesia. Tissues from infected rabbits were isolated after necropsy at 7 or 10 days after infection, fixed in neutral buffered 10% formalin, embedded in paraffin and cut into 5- μ m sections. Sections were stained with hematoxylin and eosin and viewed by light microscopy.

RESULTS

Construction of vMYX-GF⁻ΔM11L and vMYXlac. Figure 1 shows the arrangement of viral ORFs, including MGF and M11L, which map near the left terminus. Note that the orientation of the MYX genome has been reversed from that seen in previous publications (1, 12, 32, 38, 57, 58, 62) to standardize the arrangement of conserved *Leporipoxvirus* genes with those of other poxviruses (61). We have also revised our nomenclature of ORFs such that MYX ORFs mapping within the TIR will be designated M-T1 to M-T8 whereas those mapping outside the TIR will be prefaced with only M. In addition, unique ORFs are designated left (L) or right (R) to indicate their direction of transcriptional orientation. As described in Materials and Methods, we constructed a recombinant virus (vMYX-GF⁻ΔM11L) in which 460 nt, including the entire MGF coding sequence, was deleted and replaced with a β -gal cassette under the control of the vaccinia virus p11 promoter (Fig. 2). Sequencing analysis upstream of MGF (58) has indicated that an ORF homologous to an SFV ORF (originally called T11-R) (57), designated M11L, is present immediately upstream and

partially overlaps with the MGF gene (Fig. 1). These two genes are encoded within different reading frames such that the C-terminal six aa of M11L overlap the N-terminal six aa of MGF. Thus, deletion of nt sequences from the *Kpn*I site to the *Nru*I site in pMyS2a resulted in not only deletion of the entire MGF gene but also truncation of the M11L gene at the 3' end and fusion of the M11L coding sequences to the antisense orientation of the C terminus of the β -gal cassette. Since we wished to confirm that expression of the β -gal cassette itself would have no effect on the virulence or growth properties of MYX, we also constructed vMYXlac as a control virus by inserting the β -gal cassette at the *Nru*I site downstream of the MGF gene, a region that does not interrupt any ORFs or perturb the function of the M9L promoter (Fig. 2). In addition, by converting the *Bgl*II termini of the β -gal cassette into *Kpn*I sequences before insertion into the *Nru*I site of pMyS2a, the 3' junctions between the β -gal cassette and the *Nru*I site in vMYXlac and vMYX-GF⁻ΔM11L were made to contain identical nt sequences (see Materials and Methods). Thus, any possible effect of the β -gal insertion on downstream M9L gene expression would be identical in both viruses. Furthermore, to check for any effect of β -gal cassette orientation on the phenotype of the knockout recombinant, we constructed a second MGF⁻ΔM11L virus in which the β -gal cassette was inserted in the opposite orientation to that shown in Fig. 2 (not shown). The orientation of the β -gal cassette had no detectable effect on any properties of the MGF⁻ΔM11L viruses in vivo or in vitro (not shown), indicating that the

TABLE 1. Pathogenicity of MYX, vMYXlac, vMYX-GF⁻ΔM11L, vMYX-GF⁻, and vMYX-M11L⁻ in rabbits

Virus (PFU) and day	Symptom(s)	% Rabbits survived
MYX or vMYXlac (10 ³)		
5	Localized primary tumor	
9	Gram-negative infection of nasal mucosa and conjunctiva; disseminated tumors at multiple secondary sites; severe purulent conjunctivitis, rhinitis, and death	0
vMYX-GF ⁻ ΔM11L (10 ³)		
5	Localized primary tumor	
9	Primary tumor begins to regress; no secondary lesions observed; no conjunctivitis or rhinitis	
14	Complete recovery; animals immune to challenge	100
vMYX-GF ⁻ ΔM11L (10 ⁶)		
5	Localized primary tumor	
7	Slight redness of conjunctiva; occasional lesion (1–2 mm) on eyelid or ear; no conjunctivitis or rhinitis	
9	Primary tumor regresses	
14	Complete recovery; animals immune to challenge by MYX	100
vMYX-GF ⁻ (10 ³)		
5	Localized tumor	
7	Conjunctiva begin to redden	
8	Bacterial infection in conjunctiva and nares; secondary lesions appear; some animals develop labored breathing	
10–15	Primary tumors regress; 25% become moribund	75
vMYX-M11L ⁻ (10 ³)		
5	Localized protuberant tumor at inoculation site	
9	Large demarcated secondary cutaneous tumors	
15	Primary and secondary tumors reach largest size (4–5 cm, primary; 1–1.5 cm, secondary)	
15–24	Mild conjunctivitis and rhinitis	
17–21	Primary and secondary tumors regress	
40	Nearly complete recovery (remnants of tumor still present); immune to MYX challenge	100

nature of the inserted sequences fused to the M11L ORF did not affect the observed attenuated phenotype of the deletion.

Effect of the 460-nt *KpnI-NruI* deletion on MYX virulence. A total of 40 rabbits were infected i.d. with 10³ PFU of either MYX, vMYXlac, or vMYX-GF⁻ΔM11L in order to examine the effects of the deletion on the pathogenic properties of MYX during the progression of myxomatosis. Our observations are summarized in Table 1. As expected, MYX and vMYXlac recipients were indistinguishable and always developed a lethal disease characterized by large (4 to 5 cm), raised, hemorrhagic primary tumors, diffuse, swollen secondary tumors, severe purulent conjunctivitis, and rhinitis. In contrast to this, vMYX-GF⁻ΔM11L recipients remained uniformly healthy throughout the course of the infection and developed only a smaller (2 to 4 cm) nonhemorrhagic primary tumor which completely disappeared by 14 days after infection. To determine whether increased doses of vMYX-GF⁻ΔM11L could recapitulate the wild-type MYX syndrome, we infected rabbits either i.d. or intravenously with 10⁶ PFU vMYX-GF⁻ΔM11L. The only additional symptoms seen in these recipients were slight reddening of the conjunctiva and the occasional development of a small, scratchlike lesion on the eyelid or ear. We observed no signs of the purulent secondary bacterial infections, secondary tumors, conjunctivitis, or rhinitis that invariably occur in the wild-type MYX syndrome. vMYX-GF⁻ΔM11L recipients were immune to challenge with wild-type MYX at 21 days after infection. We conclude that a deletion of 460 nt encompass-

ing the MGF gene virtually abolishes the disease symptoms associated with myxomatosis and that this dramatic attenuation is neither a simple dosage effect nor is it dependent on the route of infection.

Comparative histological analysis of tissues from wild-type MYX and vMYX-GF⁻ΔM11L recipients. We examined tissue sections of primary and secondary tumors, spleen, liver, kidney, lung, conjunctiva, and nasal mucosa from MYX and vMYX-GF⁻ΔM11L recipients. The histopathological characteristics of wild-type MYX infection have been described previously (14, 18, 45, 48). A summary of the major histological differences between MYX and vMYX-GF⁻ΔM11L is presented in Table 2.

MYX recipients, day 7. The tumors seen in MYX (strain Lausanne) recipients were highly myxoid, with abundant connective tissue matrix proteins and mucopolysaccharides surrounding scattered atypical tumor cells (Fig. 3A). Compared with their counterparts in MRV-induced tumors (48), these cells were less atypical and less abundant. A slight heterophilic infiltrate within the tumor was observed. The conjunctiva in these animals show extensive squamous metaplasia and hyperplasia (Fig. 3B). In the spleen, perifollicular cell proliferation and sinusoidal congestion were observed, but the expansion of the red pulp characteristic of MRV infection was not prominent. Examination of the lungs in these animals showed no edema, though intraalveolar hemorrhage was detected.

MYX-GF⁻ΔM11L recipients, day 7. Several aspects of the

TABLE 2. Major histological differences between wild-type MYX and vMYX-GF⁻ΔM11L infection in rabbits

Virus, day, and infection site	Histological characteristic(s)
MYX	
7	
Primary tumor	Slight heterophilic infiltrate
Spleen	Prominent perifollicular hyperplasia
Conjunctiva	Squamous metaplasia and hyperplasia
11	
Primary tumor	Extensive hemorrhage; tumor mass increasing; heterophilic infiltrate
Spleen	Perifollicular hyperplasia
Conjunctiva	Squamous metaplasia and hyperplasia
vMYX-GF⁻ΔM11L	
7	
Primary tumor	Extensive lymphocytic and heterophilic infiltrate
Spleen	Prominent follicular proliferation
Conjunctiva	Normal
11	
Primary tumor	Considerable reduction of tumor mass; extensive lymphocytic and heterophilic infiltrate
Spleen	Normal
Conjunctiva	Normal

primary tumors in these animals differed greatly from observations made with wild-type MYX or vMYXlac recipients at this time point. An extensive inflammatory infiltrate was noted in myxomas from vMYX-GF⁻ΔM11L rabbits (Fig. 3C). The infiltrating cells were composed of a mixture of lymphocytes and heterophils, resembling much more the inflammation seen within and around Shope fibromas than that observed within malignant fibromas or myxomas (52). In addition, subepidermal edema at the primary site was prominent. Spleen sections from these animals showed somewhat less perifollicular hyperplasia than that seen in wild-type MYX recipients. Follicular proliferation, however, was prominent, which is indicative of a vigorous cell-mediated immune response to the viral infection. The red pulp was expanded in these animals, and sinusoids were moderately congested. Other organs examined were normal.

MYX recipients, day 11. The primary tumors in these animals showed classic myxoma tumor cells, extensive hemorrhage, and infiltration with heterophils (18). Copious amounts of extracellular matrix were deposited in areas surrounding skin appendage structures, especially hair follicles. The conjunctiva showed increased squamous metaplasia and hyperplasia, with many bizarre squamous cells in the epithelium, multiple large, atypical tumor cells in the underlying stroma, and a large, subepithelial tumor. In the spleen, the pattern of perifollicular hyperplasia was prominent, but follicular zones were unremarkable.

vMYX-GF⁻ΔM11L recipients, day 11. Much loss of primary tumor mass was observed, with considerable subepidermal edema and extensive infiltration of the tumor area by lymphocytes and heterophils (Fig. 3D). Though myxomalike tumor cells were identifiable, they were sparse and were often surrounded by a ring of heterophils and/or lymphocytes. In these respects, vMYX-GF⁻ΔM11L myxomas

closely resemble regressing Shope fibromas (52). Other organs examined from these animals were normal.

Growth of vMYX-GF⁻ΔM11L in cultured cells in vitro. The growth properties of vMYX-GF⁻ΔM11L, vMYXlac, and MYX were examined in a variety of susceptible rabbit and primate cells in vitro. In all experiments, vMYXlac and MYX behaved identically. We observed no morphological differences in the foci induced by wild-type MYX, vMYXlac, or vMYX-GF⁻ΔM11L on BGMK, SIRC, or BSC-1 cells (not shown). On RK-13 cells, however, MYX and vMYXlac produced characteristic foci, whereas vMYX-GF⁻ΔM11L lesions contained few cells in the center of the infected area and thus had a more plaque-like morphology (not shown). The growth curves of high-multiplicity (MOI = 5), single-step, productive infections of RK-13 cells by MYX and vMYX-GF⁻ΔM11L, however, were very similar (not shown). We examined the ability of MYX, vMYXlac, and vMYX-GF⁻ΔM11L to propagate through cultured cells by performing low-multiplicity (MOI = 0.002) infections in RK-13 (not shown) and SIRC cells (Fig. 4) and observed only minor differences in titers, whether or not the infected cells had been actively growing or quiescent at the time of infection (not shown).

The ability to grow in resting and mitogenically stimulated lymphocytes is crucial to the pathogenesis of MYX infection because it provides a means for impairing immune function as well as expediting dissemination in the host via the lymphatic channels (50, 51). The ability of the leporipoxviruses to propagate in cells of the immune system has been shown to correlate with the extent of pathogenicity upon infection of a susceptible host. For example, the highly virulent MRV and MYX viruses replicate efficiently in cultures of spleen cells of normal rabbits, even without mitogenic stimulation (44, 47, 50). On the other hand, SFV, a benign virus which induces only a localized primary tumor without concomitant immune suppression, is completely incapable of propagation in primary splenic cultures or in pure lymphocyte populations (20, 46). Therefore, any impediment to growth of MYX in lymphocytes as a consequence of the 460-bp deletion could in theory contribute to the observed attenuation. We examined the growth of vMYXlac and vMYX-GF⁻ΔM11L in spleen cell cultures in the presence or absence of conA stimulation at MOIs of 0.1 (not shown), 0.01 (not shown), and 0.001 (Fig. 5). At all multiplicities tested, in the presence of conA, vMYX-GF⁻ΔM11L produces substantially lower amounts of infectious progeny than vMYXlac. Even more dramatically, in the absence of conA stimulation, vMYX-GF⁻ΔM11L appears unable to replicate to any significant extent. This result suggests that resting T cells may be unable to support the replication of this deletion mutant or that replication of the mutant virus is being actively inhibited by other cell types within the splenic cell population. We conclude that vMYX-GF⁻ΔM11L is markedly restricted in its ability to grow in a mixed-lymphocyte population in vitro and suggest that the impaired ability to propagate in lymphocytes in vivo would be an important block to the spread of virus to secondary sites.

Construction and analysis of vMYX-GF⁻ with an intact M11L gene. To evaluate the effect of the MGF deletion alone in the presence of an unaltered M11L ORF, we constructed vMYX-GF⁻ as described in Materials and Methods (Fig. 2). vMYX-GF⁻ contains a β-gal cassette inserted at the BsaBI site in the middle of the MGF coding sequences (58), thereby interrupting the ORF in a fashion analogous to the SFGF disruption in MRV-GF⁻ (34). A total of 24 rabbits were infected i.d. with 10³ PFU of either MYX, vMYXlac, or vMYX-GF⁻ in order to examine the effects of the MGF

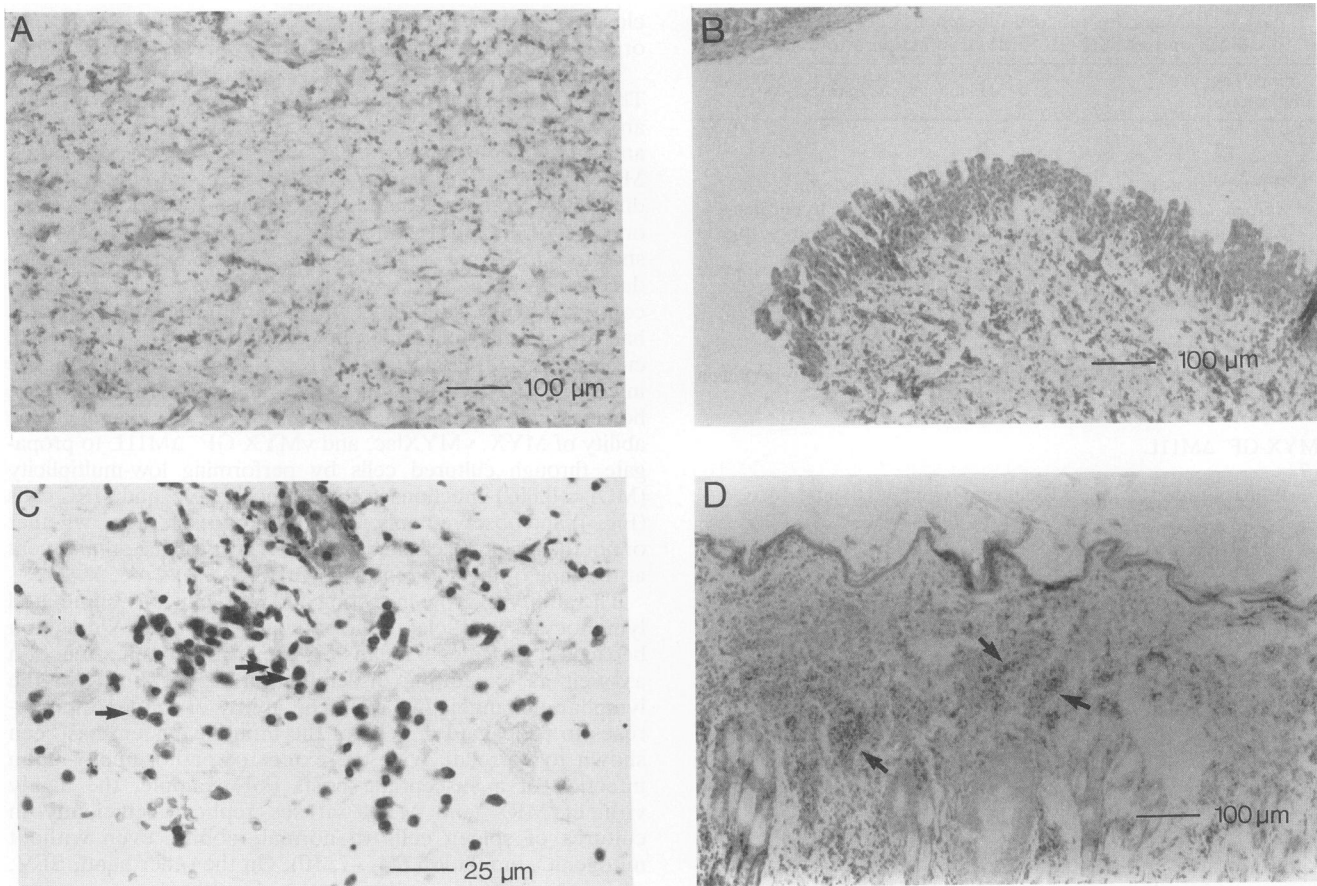


FIG. 3. (A) MYX primary tumor (day 7), composed of proliferations of fibroblasts and extensive elaboration of connective tissue matrix filaments, with an infiltrate of heterophil leukocytes. (B) MYX conjunctiva (day 7). Normally two to three cell layers thick, the epithelial layer of the conjunctiva in these rabbits has proliferated to several times its normal thickness. Underlying tumor is seen at the bottom of the frame. Conjunctiva from vMYX-GF⁻ΔM11L recipients is unaffected at both 7 and 11 days p.i. (C) vMYX-GF⁻ΔM11L primary tumor (day 7). The cells comprising these tumors are similar to those seen in wild-type tumors except that a prominent inflammatory infiltrate is noted (arrows). This type of infiltrate is absent in MYX or vMYXlac tumors. (D) vMYX-GF⁻ΔM11L primary tumor (day 11). These tumors differ from their day 7 counterparts in showing a much more prominent lymphoid infiltrate. Abundant clusters of lymphocytes (arrows) are shown.

deletion on the pathogenic properties of MYX during the progression of myxomatosis. Our observations are summarized in Table 1. The effect of interrupting MGF in MYX was indistinguishable from that resulting from inactivation of SFGF in MRV, both in vitro and in vivo (34). That is, vMYX-GF⁻ recipients developed a moderated form of myxomatosis that included the development of secondary lesions as well as bacterial infections causing purulent conjunctivitis and rhinitis. However, the disease symptoms were milder than those caused by wild-type MYX, and the majority of rabbits infected with vMYX-GF⁻ never became seriously ill. As with SFGF⁻ MRV (34), vMYX-GF⁻ infection induced myxoid primary and secondary tumors that contained fewer proliferating cells than their wild-type counterparts. Nasal mucosa and conjunctiva from vMYX-GF⁻ recipients displayed a marked reduction in the squamous metaplasia and hyperplasia that is characteristic of wild-type MRV and MYX infections. Thus, both vMYX-GF⁻ and vMRV-GF⁻ viruses are less virulent in rabbits, possibly because they induce less proliferation-induced damage to target epithelia, resulting in a reduced degree of concomitant gram-negative bacterial infections in the respiratory tract. The colony morphology of vMYX-GF⁻ was identical to those of MYX

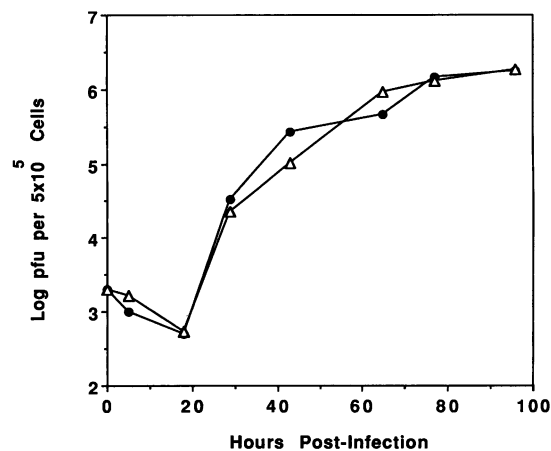


FIG. 4. Growth of vMYXlac (●) and vMYX-GF⁻ΔM11L (Δ) in tissue culture. SIRC cells were infected at an MOI of 0.004 and harvested at various times p.i., and the titers of the infectious virus on RK-13 cells were determined.

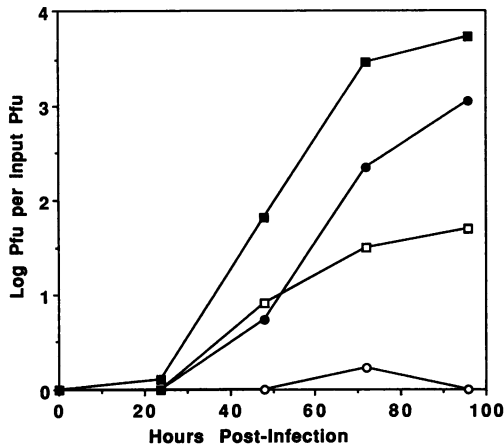


FIG. 5. Growth of vMYXlac and vMYX-GF $^{-}$ Δ M11L in primary rabbit spleen cell cultures. Cultures of spleen cells isolated from normal rabbits were infected with vMYXlac (squares) or vMYX-GF $^{-}$ Δ M11L (circles) at an MOI of 0.001 in the presence (solid symbols) or absence (open symbols) of the nonspecific T-cell mitogen conA. Cultures were harvested at various times p.i. and titered on RK-13 cells.

and vMYXlac on RK-13, SIRC, and BGMK cells (not shown), and growth curves in primary spleen cell cultures were very similar (Fig. 6). We conclude that MGF contributes to MYX pathogenicity in a fashion analogous to that of SFGF in MRV and that the extensively attenuated phenotype of vMYX-GF $^{-}$ Δ M11L is not simply due to the absence of functional MGF.

Construction of a MYX mutant with a disrupted M11L gene but an intact MGF gene. We sought to determine the contribution of M11L to the properties of MYX infection by constructing a mutant (vMYX-M11L $^{-}$) in which 53 bp between the *EcoRV* and *HincII* sites near the beginning of the M11L coding sequences was deleted and replaced with the β -gal cassette (see Materials and Methods), thereby inactivating the M11L ORF (Fig. 2). In order to confirm the genomic structure of vMYX-M11L $^{-}$, Southern blots with wild-type and recombinant vMYX-M11L $^{-}$ were performed by using the β -gal cassette and the MGF-containing, 1.5-kb MYX *HincII* fragment as probes. Digestion with diagnostic restriction enzymes such as *BglI*, *HincII*, and *SmaI* yielded the predicted products (not shown), indicating that the vMYX-M11L $^{-}$ genome does not contain an intact M11L gene and that the loss of this gene does not affect the viability of the virus in tissue culture. Western blot (immunoblot) analysis using anti-M11L antiserum indicates that cells infected with wild-type MYX and vMYXlac, but not vMYX-M11L $^{-}$, contain detectable reactive M11L protein (19), confirming that the M11L ORF has indeed been rendered nonfunctional in vMYX-M11L $^{-}$.

A total of 24 rabbits were infected i.d. with 10^3 PFU of either vMYXlac or vMYX-M11L $^{-}$ in order to examine the effects of the M11L deletion on the pathogenic properties of MYX during the progression of myxomatosis. The gross pathological observations are summarized in Table 1. vMYX-M11L $^{-}$ recipients underwent a disease course which differed substantially from vMYXlac or wild-type MYX infection. Within 6 days p.i., rabbits that had received vMYX-M11L $^{-}$ developed a local tumor at the site of inoculation that was more clearly demarcated from the surrounding skin than the corresponding lesions induced by wild-type

MYX or vMYXlac. By 8 days p.i., when vMYXlac and wild-type MYX recipients displayed marked signs of purulent bacterial infection in the conjunctiva and nasal mucosa, vMYX-M11L $^{-}$ recipients were asymptomatic in this respect. However, they developed secondary tumors which were much larger and more protuberant than corresponding wild-type lesions and were especially prominent on the eyelids. The majority (approximately 60%) of vMYX-M11L $^{-}$ recipients were completely free of secondary bacterial infections in the conjunctiva and nasal passages throughout the course of the disease, and the remainder had only mild symptoms. Those vMYX-M11L $^{-}$ recipients that did develop some bacterial infections remained asymptomatic until approximately 15 days p.i. and then exhibited only very minor signs of conjunctivitis and rhinitis. At no time during the course of the infection did any of the vMYX-M11L $^{-}$ recipients develop secondary bacterial infections or dyspnea that were comparable in severity to those characteristic of wild-type MYX or vMYXlac infection. By 17 days p.i., the vMYX-M11L $^{-}$ lesions began to regress and recovery was essentially complete by 40 days p.i. In summary, these results show that vMYX-M11L $^{-}$ is highly attenuated, indicating that the M11L gene product is important for MYX virulence.

The histopathological profile of vMYX-M11L $^{-}$ infection was conspicuously different from that of wild-type MYX or vMYXlac in several respects (Table 3). Sections of primary and secondary tumors taken from vMYX-M11L $^{-}$ recipients 10 days p.i. revealed marked vesiculation occurring within the epidermal layer of skin overlying the tumor, which was not present in tumors of vMYXlac recipients (Fig. 7A and B). The dermis in vMYX-M11L $^{-}$ tumors contained a much more prominent heterophilic infiltrate than the corresponding vMYXlac tissue, and the degree of edema was also significantly greater. Splenic macrophages of vMYX-M11L $^{-}$ recipients contained considerable granular debris, whereas this was not observed in the vMYXlac counterparts. Together, these observations suggest a more intense inflammatory reaction to vMYX-M11L $^{-}$ infection. The spleens of vMYX-M11L $^{-}$ recipients also displayed hyperplasia of the

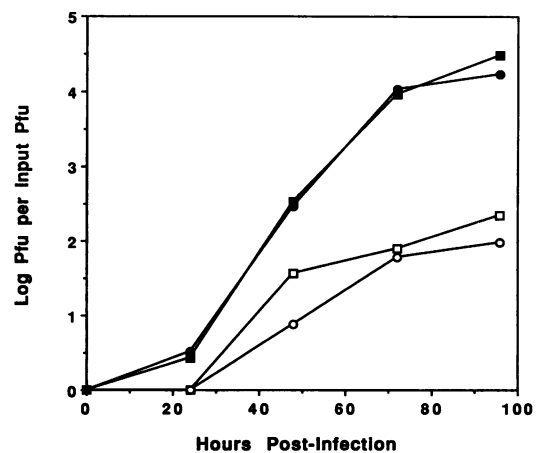


FIG. 6. Growth of vMYXlac and vMYX-GF $^{-}$ in primary rabbit spleen cell cultures. Cultures of spleen cells isolated from normal rabbits were infected with vMYXlac (squares) or vMYX-GF $^{-}$ (circles) at an MOI of 0.001 in the presence (solid symbols) or absence (open symbols) of the nonspecific T-cell mitogen conA. Cultures were harvested at various times p.i. and titered on RK-13 cells.

TABLE 3. Major histological differences between vMYXlac and vMYX-M11L⁻ infection in rabbits

Virus and site	Histological characteristic(s)
vMYXlac	
Primary and secondary tumors	Mild heterophilic infiltrate throughout dermis; no vesiculation within overlying epidermal layer; mild edema of dermis and subcutis
Spleen	Macrophages relatively quiescent and unactivated; hyperplastic periarteriolar lymphoid sheaths, with predominance of immature lymphocytes
vMYX-M11L⁻	
Primary and secondary tumors	Large numbers of infiltrating heterophil leukocytes and macrophages; marked vesiculation within overlying epidermal layer; moderate subepidermal edema
Spleen	Considerable cellular debris within cytoplasm of splenic macrophages; hyperplastic periarteriolar lymphoid sheaths, with moderate increase in percentage of immature lymphocytes

periarteriolar lymphoid sheaths, but the proportion of immature lymphocytes was markedly lower than that found in vMYXlac recipients, which indicates a lesser degree of lymphocytic depletion. No differences in the kidneys and livers of vMYXlac and vMYX-M11L⁻ recipients were observed.

Growth of vMYX-M11L⁻ in cultured cells in vitro. The growth properties of vMYX-M11L⁻ and vMYXlac were examined in rabbit kidney (RK-13) cells. Wild-type MYX and vMYXlac produced characteristic foci, whereas vMYX-M11L⁻ lesions contained fewer cells in the center of the infected area and thus had a more plaquelike morphology, which was similar to that of vMYX-GF⁻ΔM11L. We examined the ability of vMYXlac and vMYX-M11L⁻ to propagate in cultured cells by performing low-multiplicity (MOI = 0.002) infections in RK-13 cells and observed no differences in titers between the two viruses, whether or not the infected

cells were actively growing or quiescent at the time of infection (not shown).

We examined the growth of vMYXlac and vMYX-M11L⁻ in spleen cell cultures in the presence or absence of conA at an MOI of 0.001 (Fig. 8). In the presence of conA, vMYX-M11L⁻ grows to less than 10-fold-lower titers than vMYXlac. In the absence of conA stimulation, vMYX-M11L⁻ appears completely unable to propagate in these cultures. These results suggest that the inability of vMYX-GF⁻ΔM11L to propagate in unstimulated primary spleen cell cultures is due to the absence of a functional M11L gene. Thus, the M11L gene product may have a role either in virus replication in lymphocytes or in reducing the destruction of infected cells in these cultures by immune effector cells. These possibilities are presently under investigation.

DISCUSSION

The use of MYX in Australia during the 1950s as a biological control agent against feral European rabbits led to extensive investigation of the epidemiology and pathogenesis of myxomatosis (14, 18). This work has resulted in the isolation of many strains of MYX which vary substantially in virulence and in the severity of symptoms induced upon the infection of rabbits (18). To date, however, experiments using naturally occurring attenuated strains have not allowed dissection of the genetic components that contribute to the pathogenicity of MYX infection. In this study, we demonstrate that deletion of a small, defined region of the genome of a highly virulent strain of MYX (Lausanne) results in nearly complete attenuation of the viral disease. The two virulence factors whose combined inactivation appears to be responsible for the generation of this nonpathogenic phenotype are MGF, a member of the EGF family of growth factors (58), and a novel virulence marker designated M11L.

We chose to examine the role of the MGF locus in pathogenesis because other members of the EGF family, including transforming growth factor alpha, VGF, and SFGF, are known to promote cellular hyperplasia (8, 9, 28, 29, 39, 63). A synthetic peptide spanning residues 30 to 83 of the MGF gene, which includes the 6 conserved cysteine residues involved in EGF receptor binding, has also been shown to be biologically active, suggesting the *in vivo* role for this protein as an EGF receptor ligand (30). Furthermore, abrogation of VGF expression has also been found to

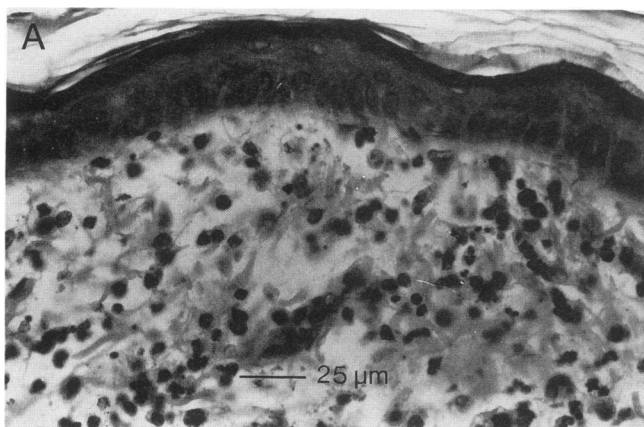


FIG. 7. Primary tumors from rabbits that had received vMYXlac (A) or vMYX-M11L⁻ (B) 9 days previously.

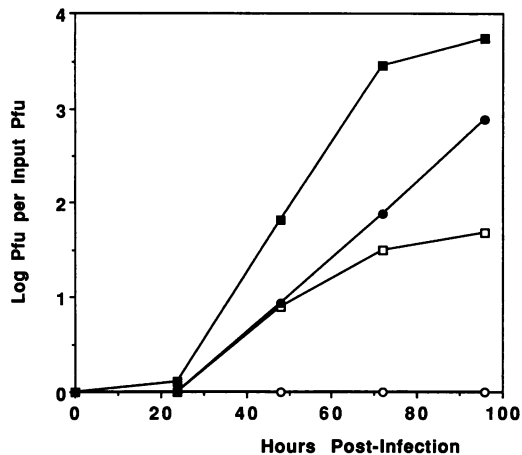


FIG. 8. Growth of vMYXlac and vMYX-M11L⁻ in primary rabbit spleen cultures. Cultures of spleen cells isolated from normal rabbits were infected with vMYXlac (squares) or vMYX-M11L⁻ (circles) at an MOI of 0.001 in the presence (solid symbols) or absence (open symbols) of conA. Cultures were harvested at various times p.i., and the titers of the virus on RK-13 cells were determined.

decrease the virulence of vaccinia virus in intracranial lethality assays of mice (5), and deletion of the SFGF gene in MRV results in moderated disease symptoms, especially conjunctivitis and rhinitis associated with epithelial metaplasia and hyperplasia at secondary sites of infection (34). In order to excise the MGF gene from the MYX genome, we made use of a unique *KpnI* site in the third codon of the MGF coding sequence and a downstream *NruI* site which maps 5' to the promoter of the adjacent gene M9L. In addition to removing the MGF locus, the 460-nt *KpnI-NruI* deletion also altered the 3' end of the upstream M11L gene because the C-terminal six aa of M11L overlap with the N terminus of MGF, although in a different reading frame. The consequence of this M11L alteration has been to truncate M11L and fuse the ORF to vector sequences from the β -gal cassette. Both orientations of the selectable marker gave virus constructs with an identical phenotype, suggesting that the pronounced attenuation of vMYX-GF⁻ Δ M11L is due to loss of both M11L and MGF functions. The possibility that additional undetected genomic alterations might be responsible for the attenuation are remote for several reasons: (i) multiple independent isolates of vMYX-GF⁻ Δ M11L resulted in the same phenotype for each clone, (ii) the orientation of the β -gal cassette in vMYX-GF⁻ Δ M11L had no effect on the phenotype, (iii) insertion of the β -gal cassette immediately downstream of MGF at the *NruI* site between MGF and M9L to generate vMYXlac had no effect on pathogenicity.

Dramatic differences between MYX and vMYX-GF⁻ Δ M11L both in vivo and in vitro were observed. Recipients of vMYX-GF⁻ Δ M11L developed a syndrome closely resembling SFV infection (32, 50), in which a primary tumor at the site of injection completely regressed by 14 days after infection, without evidence of secondary bacterial infection or any detectable compromise in immune function. Infection with very high inocula of vMYX-GF⁻ Δ M11L either i.d. or intravenously did not alter this SFV-like condition, indicating that the attenuation is indeed profound. Histologically, the tumors induced by MYX and vMYX-GF⁻ Δ M11L differ in the extent and type of inflammation present. Whereas

MYX tumors contain a mild, chiefly heterophilic inflammatory infiltrate, those of vMYX-GF⁻ Δ M11L recipients are massively infiltrated with a mixture of lymphocytes and heterophils, indicative of a more effective immune response to the virus infection. In MYX recipients, the conjunctiva displayed considerable squamous metaplasia and hyperplasia, which is thought to increase the susceptibility of such epithelia to bacterial superinfection (21, 23, 48). The lack of such epithelial alterations and indeed the absence of virtually any secondary site lesions in vMYX-GF⁻ Δ M11L recipients may partially explain the complete abrogation of the secondary bacterial infections that normally cause purulent conjunctivitis and rhinitis in these animals. In vitro, vMYX-GF⁻ Δ M11L behaved very similarly to the wild-type parent and vMYXlac in cultured cell lines, although the foci produced in RK-13 cells were rather less proliferative than those produced by the MGF⁺/M11L⁺ controls. Much more dramatically, in mitogenically stimulated spleen cell cultures, vMYX-GF⁻ Δ M11L replicated to 10-fold-lower titers than did wild-type MYX. In the absence of mitogenic stimulation, vMYX-GF⁻ Δ M11L appeared completely incapable of replication in spleen cells, whereas MYX grows well in these cultures. These results suggest that vMYX-GF⁻ Δ M11L may be impaired in its ability to propagate in lymphocytes in vivo, precluding effective dissemination of the virus via infected lymphocytes to secondary sites. Thus, it appears that the absence of induced epithelial hyperplasia and metaplasia at secondary sites of viral replication combined with the decreased capacity to disseminate through infected lymphocytes contribute greatly to the loss of virulence by vMYX-GF⁻ Δ M11L.

The attenuation displayed by vMYX-GF⁻ Δ M11L is much more severe than that expected by inactivation of MGF alone. Deletion of the growth factor gene in MRV, a virus which is closely related to MYX but instead of MGF encodes the related SFGF gene, resulted in an MRV-like syndrome of reduced severity but still qualitatively similar to that of the parent virus, except that target epithelia were less affected by the virus than those of wild-type MRV recipients, showing less severe bacterial infections and decreased squamous hyperplasia and metaplasia (34). Although 75% of MRV-GF⁻ recipients survived infection, MRV-GF⁻ was indistinguishable from wild-type MRV in in vitro assays, including colony morphology and growth in spleen cell cultures. In order to ascertain whether the more dramatic attenuation resulting from the 460-bp *KpnI-NruI* deletion in MYX could be explained by differing biological roles of MGF in MYX compared with SFGF in MRV, we inserted the β -gal cassette into the single *BsaBI* site in the middle of the MGF ORF and obtained a recombinant virus (vMYX-GF⁻) whose pathological profile was now virtually identical to that observed for MRV-GF⁻. Therefore, vMYX-GF⁻ Δ M11L is more profoundly attenuated than either MRV-GF⁻ or vMYX-GF⁻, and this attenuation cannot be attributed solely to deletion of the MGF gene alone.

These results strongly suggested that the partially overlapping M11L ORF immediately upstream of MGF is a virulence determinant in addition to MGF. Although the *KpnI-NruI* excision was constructed to remove only five aa from the M11L C terminus, this alteration directly affected M11L function. In order to confirm the possibility that alteration of the M11L ORF affected the virulence properties of vMYX-GF⁻ Δ M11L, we also constructed a unique M11L deletion mutant of MYX (vMYX-M11L⁻) in which a small portion of the M11L coding sequence was excised and replaced with a β -gal cassette, nevertheless leaving MGF

intact and functional. The properties of this virus in vivo and in vitro demonstrate that M11L is indeed an independent virulence factor in MYX. Deletion of M11L had a profound effect on the ability of MYX to propagate in primary spleen cell cultures (Fig. 8), and the in vitro growth properties in spleen cell cultures of vMYX-M11L⁻ were similar to those of vMYX-GF⁻ΔM11L. In either the presence or absence of the nonspecific T-cell mitogen conA, the productive replication of both vMYX-GF⁻ΔM11L and vMYX-M11L⁻ viruses was severely impaired in these cultures compared with that of vMYXlac or wild-type MYX. These results suggest that the M11L product is necessary for efficient growth in lymphocytes or alternatively that the absence of M11L may facilitate destruction of virus-infected cells by phagocytic or cytotoxic cells present in the spleen cell cultures.

The disease course upon infection of rabbits with vMYX-M11L⁻ is clearly attenuated compared with wild-type MYX or vMYXlac infection, since 100% of vMYX-M11L⁻ recipients survived infection whereas MYX and vMYXlac infections are invariably fatal (Table 1). vMYX-M11L⁻ recipients developed only very minor secondary bacterial infections in contrast with the severe purulent conjunctivitis and rhinitis that always accompany wild-type MYX and vMYXlac infections. Despite the mildness of vMYX-M11L⁻ infection, the protuberant tumors induced by this virus were much larger and more demarcated compared with those of vMYXlac recipients. Histological examination of primary and secondary tumors indicated that the large size of the tumors was due primarily to greater edema and massive heterophilic infiltration at sites of viral replication, rather than a more pronounced fibroblastic proliferative response. These observations, together with the much more severe dermatitis in vMYX-M11L⁻ tumors, are indicative of a strong acute inflammatory response which is not present in control vMYXlac or MYX lesions. Sections of spleens from vMYX-M11L⁻ recipients showed much less depletion of mature lymphoid cells in the periarteriolar lymphoid sheaths compared with their vMYXlac counterparts, reflecting a state of greater T-cell immune activation. The large amounts of cellular debris observed within splenic macrophages are also indicative of a more vigorous acute inflammatory activity. Together, these observations indicate a role for M11L in inhibiting the generation of a cellular immune response to viral infection at some early step, for example, the chemotactic recruitment and/or activation of infiltrating inflammatory cells. Immunofluorescence experiments (19) indicate that M11L is expressed and transported to the surface of MYX-infected cells. Importantly, M11L function is lost in vMYX-GF⁻ΔM11L because the protein does not localize at the cell surface, suggesting that the wild-type M11L protein may function by dampening an effective early inflammatory reaction. We are currently investigating whether M11L is an important virulence factor in MYX by virtue of its ability to act as a membrane-bound viroceptor (59) involved in inhibition of an early step in the development of an acute inflammatory response to viral infection. It appears clear that M11L is an important virulence factor whose effects, when combined with those of other markers such as MGF, contribute to the development of full-blown myxomatosis. The vMYX-GF⁻ΔM11L mutant described here is a dramatically attenuated form of MYX and provides the first example of a defined deletion in MYX that renders it essentially avirulent in susceptible rabbits. In addition, vMYX-GF⁻ΔM11L should provide a useful genetic background for evaluating the effects of other putative virulence factors on poxvirus pathogenesis.

ACKNOWLEDGMENTS

We thank Chido Makunike, Rob Maranchuk, and Adrian Wills for excellent technical assistance and Chris Upton for helpful discussions.

This work was supported in part by the Alberta Heritage Foundation for Medical Research (AHFMR), in part by a grant to D.S. from the Council for Tobacco Research, and by an operating grant to G.M. from the National Cancer Institute of Canada. G.M. is an AHFMR Medical Scientist, and A.O. holds an AHFMR studentship.

REFERENCES

1. Block, W., C. Upton, and G. McFadden. 1985. Tumorigenic poxviruses: genomic organization of malignant rabbit virus, a recombinant between Shope fibroma virus and myxoma virus. *Virology* **140**:113-124.
2. Bourns, M. E., I. J. Foulds, J. I. Campbell, and M. M. Binns. 1988. Non-essential genes in the vaccinia virus HindIII K fragment: a gene related to serine protease inhibitors and a gene related to the 37K vaccinia virus major envelope antigen. *J. Gen. Virol.* **69**:2995-3003.
3. Bouvier, G. 1954. Quelques remarques sur la myxomatose. *Bull. Off. Int. Epizoot.* **46**:76-77.
4. Brown, J. P., D. R. Twardzik, H. Marquardt, and G. J. Todaro. 1985. Vaccinia virus encodes a polypeptide homologous to epidermal growth factor and transforming growth factor. *Nature (London)* **313**:491-492.
5. Buller, R. M., S. Chakrabarti, J. A. Cooper, D. R. Twardzik, and B. Moss. 1988. Deletion of the vaccinia virus growth factor gene reduces virus virulence. *J. Virol.* **62**:866-874.
6. Buller, R. M., S. Chakrabarti, B. Moss, and T. Fredrickson. 1988. Cell proliferative response to vaccinia virus is mediated by VGF. *Virology* **164**:182-192.
7. Buller, R. M. L., and G. J. Palumbo. 1991. Poxvirus pathogenesis. *Microbiol. Rev.* **55**:80-122.
8. Burgess, A. W. 1989. Epidermal growth factor and transforming growth factor α . *Br. Med. Bull.* **45**:401-424.
9. Carpenter, G., and S. Cohen. 1990. Epidermal growth factor. *J. Biol. Chem.* **265**:7709-7712.
10. Chakrabarti, S., K. Brechling, and B. Moss. 1985. Vaccinia virus expression vector: coexpression of beta-galactosidase provides visual screening of recombinant virus plaques. *Mol. Cell Biol.* **5**:3403-3409.
11. Chambers, S. P., S. E. Prior, D. A. Barstow, and N. P. Minton. 1988. The pMTL nic⁻ cloning vectors. I. Improved pUC poly-linker regions to facilitate the use of sonicated DNA for nucleotide sequencing. *Gene* **68**:139-149.
12. Chang, W., C. Upton, S. L. Hu, A. F. Purchio, and G. McFadden. 1987. The genome of Shope fibroma virus, a tumorigenic poxvirus, contains a growth factor gene with sequence similarity to those encoding epidermal growth factor and transforming growth factor α . *Mol. Cell Biol.* **7**:535-540.
13. DeLange, A. M., M. Reddy, D. Scraba, C. Upton, and G. McFadden. 1986. Replication and resolution of cloned poxvirus telomeres in vivo generates linear minichromosomes with intact viral hairpin termini. *J. Virol.* **59**:249-259.
14. Fenner, F. 1990. Poxviruses of laboratory animals. *Lab. Anim. Sci.* **40**:469-480.
15. Fenner, F. 1990. Poxviruses, p. 2113-2133. *In* B. N. Fields and D. M. Knipe (ed.), *Virology*. Raven Press, New York.
16. Fenner, F., and F. M. Burnet. 1957. A short description of the pox-virus group (vaccinia and related viruses). *Virology* **4**:305-314.
17. Fenner, F., and I. D. Marshall. 1957. A comparison of the virulence for European rabbits (*Oryctolagus cuniculus*) of strains of myxoma virus recovered in the field in Australia, Europe, and America. *J. Hyg.* **55**:149-191.
18. Fenner, F., and F. N. Ratcliffe. 1965. *Myxomatosis*. Cambridge University Press, London.
19. Graham, K. A., A. Opgenorth, C. Upton, and G. McFadden. Submitted for publication.
20. Heard, H. K., K. O'Connor, and D. S. Strayer. 1990. Molecular analysis of immunosuppression induced by virus replication in

- lymphocytes. *J. Immunol.* **144**:3992–3999.
21. **Heath, R. B.** 1979. The pathogenesis of respiratory viral infections. *Postgrad. Med. J.* **55**:122–127.
 22. **Innis, M. A., D. H. Gelfand, J. J. Sninsky, and T. J. White.** 1990. PCR protocols. Academic Press, San Diego, Calif.
 23. **Jakab, G. J., G. A. Warr, and M. E. Knight.** 1979. Pulmonary and systemic defenses against challenge with *Staphylococcus aureus* in mice with pneumonia due to influenza A virus. *J. Infect. Dis.* **140**:105–108.
 24. **King, C. S., J. A. Cooper, B. Moss, and D. R. Twardzik.** 1986. Vaccinia virus growth factor stimulates tyrosine protein kinase activity of A431 cell epidermal growth factor receptors. *Mol. Cell. Biol.* **6**:332–336.
 25. **Kotwal, G. J., S. N. Isaacs, R. McKenzie, M. M. Frank, and B. Moss.** 1990. Inhibition of the complement cascade by the major secretory protein of vaccinia virus. *Science* **250**:827–830.
 26. **Kotwal, G. J., and B. Moss.** 1988. Vaccinia virus encodes a secretory polypeptide structurally related to complement control proteins. *Nature (London)* **335**:176–178.
 27. **Kotwal, G. J., and B. Moss.** 1989. Vaccinia virus encodes two proteins that are structurally related to members of the plasma serine protease inhibitor superfamily. *J. Virol.* **63**:600–606.
 28. **Laurence, D. J. R., and B. A. Gusterson.** 1990. The epidermal growth factor. *Tumor Biol.* **11**:229–261.
 29. **Lin, Y. Z., G. Caporaso, P. Y. Chang, X. H. Ke, and J. P. Tam.** 1988. Synthesis of a biological active tumor growth factor from the predicted DNA sequence of Shope fibroma virus. *Biochemistry* **27**:5640–5645.
 30. **Lin, Y. Z., X. H. Ke, and J. P. Tam.** 1991. Synthesis and structure-activity study of myxoma virus growth factor. *Biochemistry* **30**:3310–3314.
 31. **Maré, C. J.** 1974. The biology of the laboratory rabbit, p. 237–261. Academic Press, Inc., New York.
 32. **McFadden, G.** 1988. Poxviruses of rabbits, p. 37–62. *In* G. Darai (ed.), *Virus diseases in laboratory and captive animals*. Martinus Nijhoff Publishers, Boston.
 33. **Moss, B.** 1990. Poxviridae and their replication, p. 2079–2111. *In* B. N. Fields and D. M. Knipe (ed.), *Virology*. Raven Press, New York.
 34. **Oggenorth, A., D. Strayer, C. Upton, and G. McFadden.** 1992. Deletion of the growth factor gene related to EGF and TGF α reduces virulence of malignant rabbit fibroma virus. *Virology* **186**:175–191.
 35. **Pickup, D. J., B. S. Ink, W. Hu, C. A. Ray, and W. K. Joklik.** 1986. Hemorrhage in lesions caused by cowpox virus is induced by a viral protein that is related to plasma protein inhibitors of serine proteases. *Proc. Natl. Acad. Sci. USA* **83**:7698–7702.
 36. **Porter, C. D., and L. C. Archard.** 1987. Characterization and physical mapping of *Molluscum contagiosum* virus DNA and location of a sequence capable of encoding a conserved domain of epidermal growth factor. *J. Gen. Virol.* **68**:673–682.
 37. **Porter, C. D., N. W. Blake, and L. C. Archard.** 1988. Structure and activity of epidermal-growth-factor-like peptides: induction of basal cell proliferation by a poxvirus gene product? *Biochem. Soc. Trans.* **16**:671–674.
 38. **Russell, R. J., and S. J. Robbins.** 1989. Cloning and molecular characterization of the myxoma virus genome. *Virology* **170**:147–159.
 39. **Salomon, D. S., N. Kim, T. Saeki, and F. Ciardiello.** 1990. Transforming growth factor- α : an oncogene developmental growth factor. *Cancer Cells* **2**:389–397.
 40. **Sambrook, J., E. F. Fritsch, and T. Maniatis.** 1989. *Molecular cloning: a laboratory manual*. Cold Spring Harbor Laboratory Press, Cold Spring Harbor, N.Y.
 41. **Sanes, J. R., J. L. R. Rubenstein, and J.-F. Nicolas.** 1986. Use of a recombinant retrovirus to study post-implantation cell lineage in mouse embryos. *EMBO J.* **5**:3133–3142.
 42. **Smith, C. A., T. Davis, J. M. Wignall, W. S. Din, T. Farrah, C. Upton, G. McFadden, and R. G. Goodwin.** 1991. T2 open reading frame from the Shope fibroma virus encodes a soluble form of the TNF receptor. *Biochem. Biophys. Res. Commun.* **176**:335–342.
 43. **Smith, G. L., S. T. Howard, and Y. S. Chan.** 1989. Vaccinia virus encodes a family of genes with homology to serine proteinase inhibitors. *J. Gen. Virol.* **70**:2333–2343.
 44. **Strayer, D. S.** 1988. Poxviruses, p. 173–192. *In* S. Specter, M. Bendinelli, and H. Friedmann (ed.), *Virus-induced immunosuppression*. Plenum Press, New York.
 45. **Strayer, D. S., G. Cabirac, S. Sell, and J. L. Leibowitz.** 1983. Malignant rabbit fibroma virus: observations on the culture and histopathologic characteristics of a new virus-induced rabbit tumor. *JNCI* **71**:91–104.
 46. **Strayer, D. S., K. A. Laybourn, and H. K. Heard.** 1990. Determinants of the ability of malignant fibroma virus to induce immune dysfunction and tumor dissemination *in vivo*. *Microb. Pathog.* **9**:173–189.
 47. **Strayer, D. S., and J. L. Leibowitz.** 1987. Virus-lymphocyte interactions during the course of immunosuppressive virus infection. *J. Gen. Virol.* **68**:463–472.
 48. **Strayer, D. S., and S. Sell.** 1983. Immunohistology of malignant rabbit fibroma virus—a comparative study with rabbit myxoma virus. *JNCI* **71**:105–116.
 49. **Strayer, D. S., S. Sell, E. Skaletsky, and J. L. Leibowitz.** 1983. Immunologic dysfunction during viral oncogenesis. I. Nonspecific immunosuppression caused by malignant rabbit fibroma virus. *J. Immunol.* **131**:2595–2600.
 50. **Strayer, D. S., E. Skaletsky, and J. L. Leibowitz.** 1985. *In vitro* growth of two related leporipoxviruses in lymphoid cells. *Virology* **145**:330–334.
 51. **Strayer, D. S., E. Skaletsky, J. L. Leibowitz, and J. Dombrowski.** 1987. Growth of malignant rabbit fibroma virus in lymphoid cells. *Virology* **158**:147–157.
 52. **Strayer, D. S., E. Skaletsky, and S. Sell.** 1984. Strain differences in Shope fibroma virus. An immunopathologic study. *Am. J. Pathol.* **116**:342–358.
 53. **Stroobant, P., A. P. Rice, W. J. Gullick, D. J. Cheng, I. M. Kerr, and M. D. Waterfield.** 1985. Purification and characterization of vaccinia virus growth factor. *Cell* **42**:383–393.
 54. **Traktman, P.** 1990. Poxviruses: an emerging portrait of biological strategy. *Cell* **62**:621–626.
 55. **Turner, P. C., and R. W. Moyer.** 1990. The molecular pathogenesis of poxviruses. *Curr. Top. Microbiol. Immunol.* **163**:125–152.
 56. **Twardzik, D. R., J. B. Brown, J. E. Ranchalis, G. J. Todaro, and B. Moss.** 1985. Vaccinia virus-infected cells release a novel polypeptide functionally related to transforming and epidermal growth factors. *Proc. Natl. Acad. Sci. USA* **82**:5300–5304.
 57. **Upton, C., J. L. Macen, R. A. Maranchuk, A. M. DeLange, and G. McFadden.** 1988. Tumorigenic poxviruses: fine analysis of the recombination junctions in malignant rabbit fibroma virus, a recombinant between Shope fibroma virus and myxoma virus. *Virology* **166**:229–239.
 58. **Upton, C., J. L. Macen, and G. McFadden.** 1987. Mapping and sequencing of a gene from myxoma virus that is related to those encoding epidermal growth factor and transforming growth factor alpha. *J. Virol.* **61**:1271–1275.
 59. **Upton, C., J. L. Macen, M. Schreiber, and G. McFadden.** 1991. Myxoma virus expresses a secreted protein with homology to the tumor necrosis factor receptor gene family that contributes to viral virulence. *Virology* **184**:370–382.
 60. **Upton, C., J. L. Macen, D. S. Wishart, and G. McFadden.** 1990. Myxoma virus and malignant rabbit fibroma virus encode a serpin-like protein important for virus virulence. *Virology* **179**:618–631.
 61. **Upton, C., A. Oggenorth, P. Traktman, and G. McFadden.** 1990. Identification and DNA sequence of the Shope fibroma virus DNA topoisomerase gene. *Virology* **176**:439–447.
 62. **Wills, A., A. M. DeLange, C. Gregson, C. Macaulay, and G. McFadden.** 1983. Physical characterization and molecular cloning of the Shope fibroma virus DNA genome. *Virology* **130**:403–414.
 63. **Ye, Y. K., Y. Z. Lin, and J. P. Tam.** 1988. Shope fibroma virus growth factor exhibits epidermal growth factor activities in newborn mice. *Biochem. Biophys. Res. Commun.* **154**:497–501.